Journal of Applied Electrochemistry (2006) 36:983–989
DOI 10.1007/s10800-006-9128-9

A non-linear AC spectrometry study of the electrodeposition of Cu from acidic sulphate solutions in the presence of PEG

BENEDETTO BOZZINI[1,*] and IVONNE SGURA[2]
[1]*Dipartimento di Ingegneria dell'Innovazione, Università di Lecce, via Monteroni, I-73100 Lecce, Italy*
[2]*Dipartimento di Matematica, Università di Lecce, via Arnesano, I-73100 Lecce, Italy*
*(*author for correspondence, e-mail: benedetto.bozzini@unile.it)*

Received 8 September 2005; accepted in revised form 18 January 2006

Abstract

Non-linear Alternated-Current (AC) spectrometry has been recently proposed [Bozzini and Sgura, *Math. Prob. Eng*. (in press)] as an approach able to yield basically the same results as AC impedance spectroscopy, but with a remarkably higher statistical confidence. In particular, quantitative parameter estimation problems commonly found in the analysis of AC impedance data carried out with the available methods [Sgura and Bozzini, *J. Non-Lin. Mech*. **40** (2005) 557], can be remarkably reduced. This paper reports the first example of the experimental implementation of the method, as applied to Cu electrodeposition from a sulphate solution containing polyethyleneglycol, a system relevant to semiconductor fabrication, previously investigated by electrochemical and spectroelectrochemical methods in our group [Bozzini et al. *J. Appl. Electrochem*. (in press), Bozzini et al. *J. Appl. Electrochem*. **36** (2006) 87].

1. Introduction

Electrodeposition of Cu from acidic sulphate solutions has experienced renewed interest in the last decade, owing to expanding applications in the miniaturised fabrication of semiconductor devices. Polyethyleneglycol (PEG) is well known to play a critical role in the electrodeposition of Cu from acidic sulphate solutions [1, 2]. This polymer acts as a suppressor and operates synergistically with accelerators for the achievement of optimal superfilling of vias and trenches and the minimisation of bump formation in semiconductor microfabrication processes. Previous investigations in our group, carried out by *in situ* surface-enhanced Raman and electroreflectance spectroscopies and cyclic voltammetry, highlighted some aspects of the adsorption behaviour and cathodic reactivity of PEG and its electrokinetic effects. PEG has been found to complex Cu^{+} and Cu^{2+} and thus to impact the electroreduction kinetics, in particular the charge-transfer process appears to be enhanced by the presence of PEG in Cl^{-}-free solutions [1]. Cyclic voltammetry carried out with a rotating disk electrode showed that the synergy of PEG and Cl^{-} can be explained in terms of changes in adsorption mode: Cl^{-} acts as a spacer between the metal and the polymer layer.

In situ surface-enhanced Raman spectroscopy carried out during Cu electrodeposition proved PEG adsorption and cathodic reactivity implying polymer fragmentation and formation of vinyl ether groups; the suppressor activity of the polymer can be related to its particular interfacial behaviour. In [2] it was shown, on the basis of in situ electroreflectance spectroscopy performed during Cu electrodeposition, that the optical properties of Cu are altered by the presence of PEG in a way that implies an enhancement of spectral reflectivity as electrodeposition time lapses; this behaviour was explained with the growth of a more compact metal layer in the presence of the polymer.

The cathodic electrokinetics of Cu electrodeposition in the presence PEG and other organic additives warrant further investigation [3].

Alternated Current (AC) impedance spectroscopy is the approach of choice for the evaluation of kinetic constants, but the mathematical apories of fitting impedance loci to kinetic models [4] jeopardises the attempt to extract quantitative data from experimental results. In fact, in [4] we proved that parameter identification procedures based on classical Total Electrochemical Impedance (TEI) are generally ill-posed problems; this implies that several and different sets of optimal parameters with low residuals are found, yielding numerically undistinguishable spectra. We defined these sets Numerical Global Minima (NGM).

To circumvent these problems, we have introduced a mathematical formulation for the TEI that accounts for non-linear effects in AC electrochemical measurements [5]. In fact, based on the Fourier expansion of the

Faradaic Electrochemical Impedance (FEI) up to the *m*-th harmonic term, we introduced the corresponding definition of TEI that incorporates nonlinearities [5]. By considering a very simple differential model for the dynamics of a system of two electrochemical reactions with Tafel kinetics (four parameters: two exchange current densities and two Tafel slopes) (e.g. [6]), an estimate of truncation error decay and the analytical expressions for each harmonic term (magnitude and phase) are obtained. It is worth noting that the first harmonic or linear terms correspond to classical forms of FEI and TEI, respectively. (Of course, the term "impedance" in the strict sense implies linearity; we retained this term also in the non-linear case, where "transfer function" would have been more correct, for historical and reference reasons.)

Moreover, working on simulated data, we have shown that non uniqueness in parameter identification can be removed by considering higher harmonic terms of TEI as a regularization tool to filter out the best NGM candidate [5].

In this paper, we present the first experimental results concerning electrokinetic parameter extraction using the above non-linear AC spectrometry approach, obtained with a specially designed Frequency Response Analyser (FRA).

2. Experimental

The electrodeposition bath was: $CuSO_4 \cdot 5H_2O$ 20 mM, H_2SO_4 0.5 M and PEG MW 1500, 2 g l^{-1}. The solution was prepared from analytical grade chemicals and ultrapure water with a resistivity of 18.2 MΩ cm. The solutions were degassed by bubbling with nitrogen and the electrolyte was maintained under a nitrogen blanket during the measurements. Electrochemical measurements were performed with a modified version of an AMEL system for AC impedance, based on a 7050 potentiostat and a 7200 FRA, build by AMEL according to our electronic and software design. An Ag/AgCl (KCl 3M) reference electrode was employed. A PAR Model 636 rotating-disk electrode (RDE) was used, and experiments were carried out at a rotation rate of 1000 rpm.

3. Essential mathematical notations and definitions

In this section, we briefly recall the mathematical expressions of *FEI and TEI up to the m-th harmonic* given in [5]. If Z_F^{-1} is the Faradaic Electrochemical Impedance, the following expansion can be considered:

$$Z_F^{-1} = \sum_{k=1}^{m} (Z_F^{-1})^{(k)} + R_{m+1} = Z_{Fm}^{-1} + R_{m+1}, \tag{1}$$

where R_{m+1} is the remainder corresponding to the *m*-th order of approximation. The term Z_{Fm}^{-1} is defined as *the FEI up to the m-th harmonic*.

Since, by definition, the Total Electrochemical Impedance (TEI) Z_{TOT} is given by

$$Z_{TOT} = R_0 + \frac{1}{Z_F^{-1} + i\omega C}, \tag{2}$$

we define as Z_{TOTm} the *TEI up to the m-th harmonic* the following approximation of Z_{TOT} obtained by considering in the Equation (2) the expression of Z_F^{-1} given in (1), that is

$$Z_{TOT} \approx Z_{TOTm} = R_0 + \frac{1}{Z_{Fm}^{-1} + i\omega C}. \tag{3}$$

In this paper we employed the simplest literature model (e.g. [6]) able to account for the observed (first-harmonic) impedance spectra and compatible with literature reaction models for the acidic sulphate system (e.g. [7]). It is worth noting that the use of complex reaction schemes, often found in the literature, to explain impedance loci that can be followed with simpler models, of course further reduces the statistical confidence of the parameters identified; furthermore, inspection of many published values suggests that such parameter values were not derived from a numerical minimisation, but rather fixed. In this way no information on the statistical confidence of the estimation can be derived from the experimental data.

The model chosen is thus:

$$Cu_{aq}^{2+} + e^- \rightarrow Cu_{ads}^{+}, \tag{4}$$

$$Cu_{aq}^{+} + e^- \rightarrow Cu, \tag{5}$$

by Cu_{aq}^{2+} we mean a Cu(II) species in the aqueous phase, possibly complexed by an organic ligand, not necessarily an aquocomplex; similarly Cu_{ads}^{+} denotes Cu(I) species adsorbed at the cathode and possibly coadsorbed with ligands or their reaction products. The mass balance on the coverage degree with Cu_{ads}^{+}, $\vartheta = \Gamma(Cu_{ads}^{+})/\Gamma_{max}$ (Cu_{ads}^{+}), where Γ indicates the surface concentration, is thus written as:

$$\begin{cases} \beta \dfrac{d\vartheta}{dt} = A_1(1-\vartheta) - A_2\vartheta, \\ \vartheta(0) = 0, \end{cases} \tag{6}$$

where, assuming Tafel electrokinetics, as customary in electrochemical impedance modelling (e.g. [6]):

$$A_1 = a_1 e^{b_1 \bar{\eta}}, \tag{7}$$

$$A_2 = a_2 e^{b_2 \bar{\eta}}, \tag{8}$$

the pedices "1" and "2" refer to the kinetic Equations (4) and (5), respectively, $\bar{\eta}>0$ is the overvoltage, a_i are the exchange current densities, b_i are the Tafel slopes and β is a normalisation constant accouting for the dimensionality of the balance equation.

Electrochemical impedance measurements are typically carried out by recording the response of the system to an applied sinusoidal perturbation $\delta\eta = \Delta\eta e^{i\omega t}$ of amplitude $\Delta\eta$ and frequency ω added to the constant potential $\bar{\eta}$ and varying the angular frequency ω in a given range.

After some analytical and algebraic manipulations, we can provide the analytical forms of the single harmonics of the FEI and TEI (for details, see [5]) as a function of ω and of the kinetic parameters array $p=[a_1, a_2, b_1, b_2]$, to be identified.

Hence, assuming for simplicity that the ohmic resistance $R_0=0\Omega$, we rewrite the above Equations (2) and (3) as follows:

$$Z_{\mathrm{TOT}}(\omega) = \frac{1}{S(\omega)+R_{m+1}} \approx Z_{\mathrm{TOTm}}(\omega) := \frac{1}{S(\omega)} := \frac{1}{S_1 + S_2 q + S_3 q^2 + \cdots + S_m q^{m-1}}, \quad (9)$$

where

$$q = \alpha\Delta\eta, \text{ with } \alpha = (A_1 b_1 + A_2 b_2)/\beta. \quad (10)$$

The terms $S_k \equiv S_k(\omega)$, $k=1,\ldots,m$ can be calculated by using the mathematical expressions for the components $(Z_{\mathrm{F}}^{-1})^{(k)}$, $k=1,\ldots,m$ in Equation (1) and derived in [5] by means of the Fourier analysis. Hence, the following expressions hold:

$$\begin{cases} S_1 := (Z_{\mathrm{F}}^{-1})^{(1)} + i\omega C = \frac{1}{R_t} + f_1(\omega) e^{i\varphi_1(\omega)} + i\omega C, \\ f_1(\omega) = \frac{\xi}{a^2+\omega^2}, \quad e^{i\varphi_1(\omega)} = a - i\omega, \end{cases} \quad (11)$$

$$\begin{cases} S_k := (Z_{\mathrm{F}}^{-1})^{(k)} = f_k(\omega) e^{i\varphi_k(\omega)} \\ \qquad = f_k(\omega)(\cos(\varphi_k(\omega)) + i\sin(\varphi_k(\omega)), \\ f_k(\omega) = \frac{f_1(\omega)}{\prod_{n=2}^{k}(a^2+n^2\omega^2)}, \quad 2 \leqslant k \leqslant m, \end{cases} \quad (12)$$

where the phases φ_k are given by the following recurrence relation

$$e^{i\varphi_k(\omega)} = (-1)^{k-1} \prod_{n=1}^{k} (a - in\omega), \quad 2 \leqslant k \leqslant m. \quad (13)$$

Therefore, it is easy to obtain the expression up to the m-th harmonic of the TEI in the complex field as:

$$Z_{\mathrm{TOTm}}(\omega) = Z_1(\omega) + Z_2(\omega) + \cdots + Z_m(\omega), \quad (14)$$

with

$$Z_k(\omega) = \frac{\overline{S}_k q^{k-1}}{|S(\omega)|^2}, \quad 1 \leqslant k \leqslant m, \quad (15)$$

where the "bar" indicates the complex conjugate value of S_k and $|S(\omega)|^2$ the squared modulus of $S(\omega)$.

For the other parameters appearing in the above formulae (11)–(12)–(13), the following relations hold:

$$\begin{aligned} a &= (A_1 + A_2)/\beta, \\ 1/R_t &= FA_1A_2(b_1 + b_2)/(A_1 + A_2), \\ \beta\xi &= FA_1A_2(b_1 - b_2)(A_2 - A_1)/(A_1 + A_2). \end{aligned} \quad (16)$$

The quantities $F=96500$ C mol^{-1} and $\beta=2.7$ nmol cm^{-2} are known constants, C can be assumed to be a constant with a typical value of 25 μF cm^{-2}.

Finally, in terms of previous notation, the remainder R_{m+1} of the Faradaic Impedance truncated at the m-th term in Equation (9) is given by

$$R_{m+1} = \sum_{k=m+1}^{\infty} S_k q^{k-1} \quad (17)$$

and satisfies the condition (see [5] for the proof):

$$\max_{\omega}|R_{m+1}(\omega)| \leqslant O(q^m/(m+1)!).$$

Then, even if q given in (10) is parameter-dependent, the remainder is expected to go to zero very quickly.

4. Results and discussion

Non-linear AC experiments were run at −50 and −250 mV vs Ag/AgCl, the potential modulation $\Delta\eta$ was 30 mV and the frequency range 300 kHz–0.4 Hz. The corresponding impedance loci are plotted as circles in Figures 1 and 2, respectively; the moduli of second and third harmonics are plotted as circles in Figures 3 and 4.

We apply a Non-linear Least Squares fitting procedure based on the classical TEI (i.e. $m=1$) to the experimental data of Figures 1 and 2, with one thousand

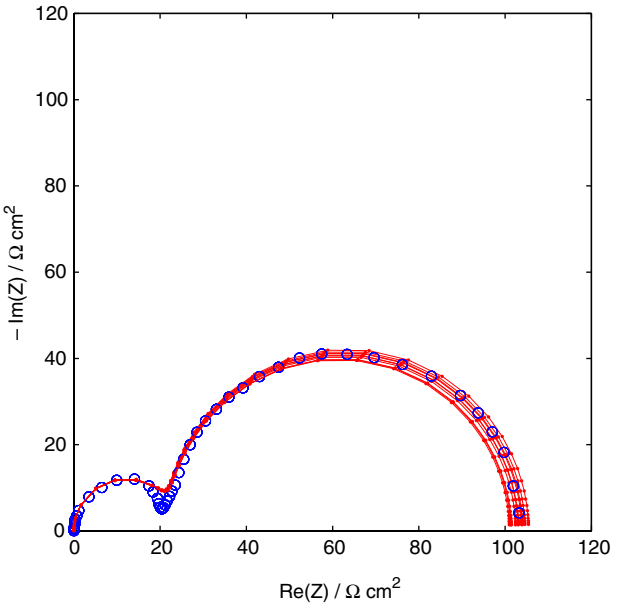

Fig. 1. Measured (circles) and fitted (line + symbol) impedance loci: baseline potential −50 mV(Ag/AgCl), frequency range 300 kHz–0.4 Hz, potential modulation amplitude 30 mV.

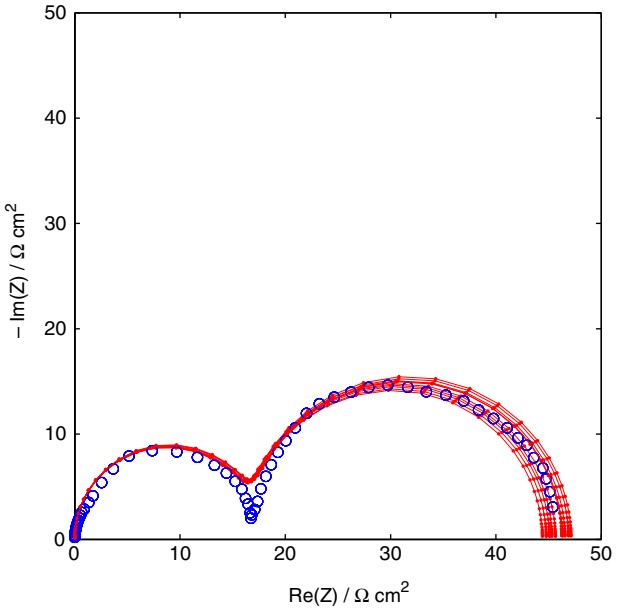

Fig. 2. Measured (circles) and fitted (line + symbol) impedance loci: baseline potential −250 mV(Ag/AgCl), frequency range 300 kHz–0.4 Hz, potential modulation amplitude 30 mV.

random initial guesses of the parameters in the range $\Omega_a \times \Omega_b = [1 \times 10^{-3}\ \text{mA cm}^{-2},\ 10\ \text{mA cm}^{-2}] \times [1\ \text{mV dec}^{-1},\ 2500\ \text{mV dec}^{-1}]$. The algorithm used is based on the *lsqcurvefit.m* routine in the *Optimization Toolbox* of *Matlab* [8]. According to the definition given in [4], for the two experiments discussed, we found the NGMs reported in Tables 1 and 2.

The spectra corresponding to the NGMs reported in Tables 1 and 2 are reported in Figures 1 and 2 as line plots; the different NGMs correspond essentially to equivalent fitting results.

In order to apply our regularisation tool based on higher harmonic models of TEI, we have to decide which order of approximation m has to be considered. This choice can be driven by two main factors: noise limits of the experimental set-up and estimate of the remainder in the Impedance expansion. In this case, we choose m such that the following estimate for the maximum truncation error T_{m+1} holds:

$$T_{m+1} := \max_{\omega} |R_{m+1}(\omega; p)| < \text{tol}, \tag{18}$$

where tol is a fixed tolerance.

The estimates of T_{m+1} in (18) for each NGM corresponding to experiments carried out at −50 and −250 mV vs Ag/AgCl are given in Tables 3 and 4. In this work we set $\text{tol} = 1.0 \times 10^{-6}$, the reason for this choice is that – from the experimental point of view – it corresponds to measured voltages ca. 4 orders of magnitude lower than the first harmonic. In these conditions the available electronics are not able to discriminate between signal and noise and consequently the numerical model would have no observable counterpart. Since in all cases of both experiments the truncation error tends quickly to zero for $m + 1 \geqslant 4$, these

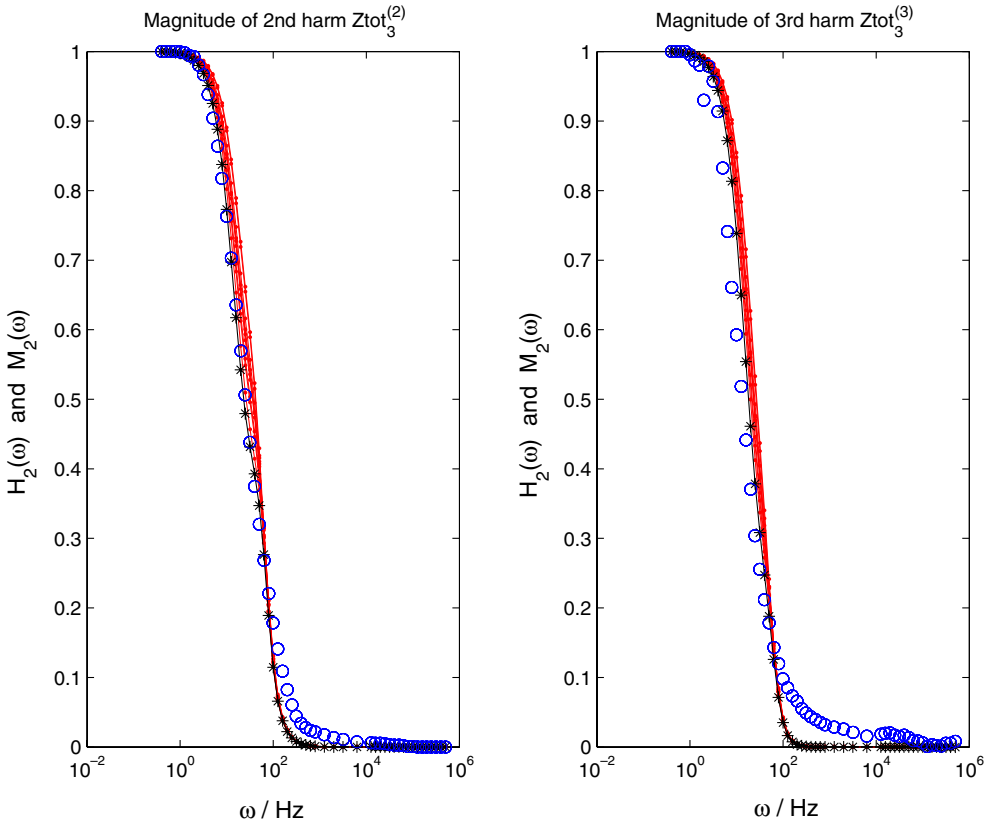

Fig. 3. Measured (circles) and theoretical (line + symbol) magnitudes of the second (left) and third (right) harmonics: baseline potential −50 mV(Ag/AgCl), frequency range 300 kHz–0.4 Hz, potential modulation amplitude 30 mV.

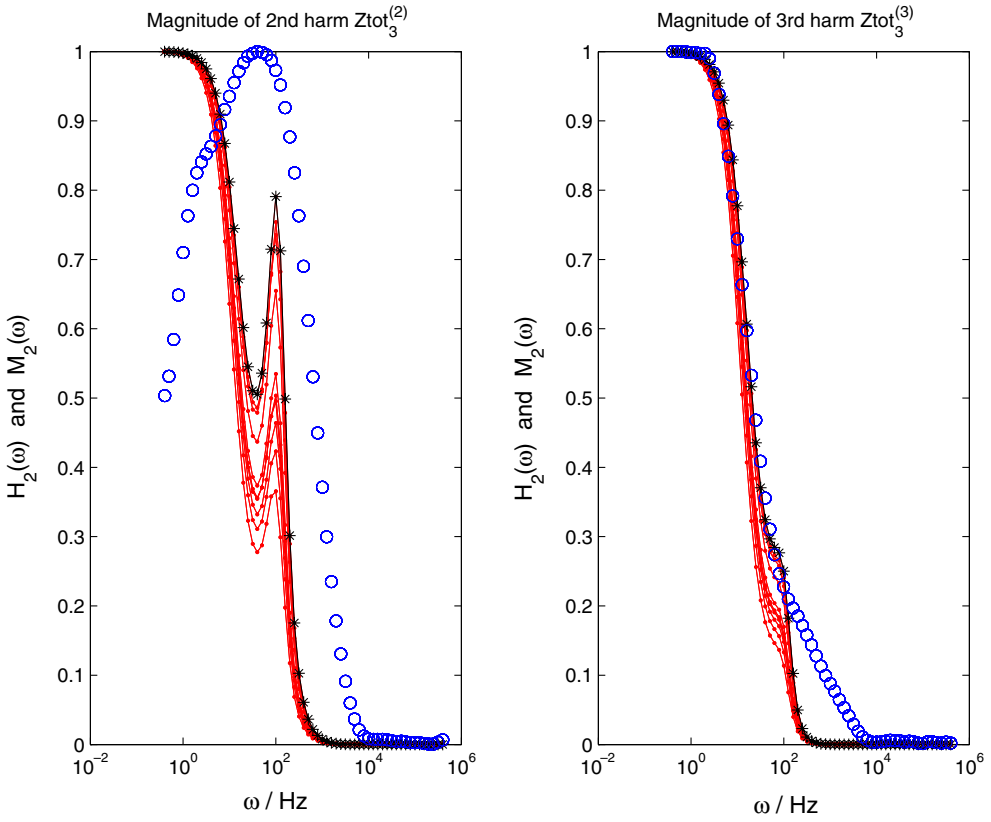

Fig. 4. Measured (circles) and theoretical (line + symbol) magnitudes of the second (left) and third (right) harmonics: baseline potential −250 mV(Ag/AgCl), frequency range 300 kHz–0.4 Hz, potential modulation amplitude 30 mV.

Table 1. The 10 Numerical Global Minima with lowest residues extracted from 1000 converged Non-Linear Least-Squares fits of impedance loci measured at baseline potential −50 mV(Ag/AgCl)

$\mathbf{p}^{(k)}_{NGM}$	a_1/mA cm^{-2}	a_2/mA cm^{-2}	b_1/mV dec^{-1}	b_2/mV dec^{-1}
1	3.064	2.0646E-2	2.9896	1572.9
2	2.9304	1.8582E-2	8.0208	1588.9
3	2.2634	9.3431E-3	38.028	1748.3
4	2.0754	7.3204E-3	48.249	1795.8
5	1.9931	6.4446E-3	52.946	1835.4
6	1.9096	5.6781E-3	57.931	1864.5
7	1.6825	3.8434E-3	73.094	1948.1
8	1.6106	3.3708E-3	78.419	1970.1
9	1.3687	1.9482E-3	97.713	2110.1
10	1.2158	1.2736E-3	113.54	2188.6

Table 2. The 10 Numerical Global Minima with lowest residues extracted from 1000 converged Non-Linear Least-Squares fits of impedance loci measured at baseline potential −250 mV(Ag/AgCl)

$\mathbf{p}^{(k)}_{NGM}$	a_1/mA cm^{-2}	a_2/ mA cm^{-2}	b_1/ mV dec^{-1}	b_2/ mV dec^{-1}
1	5.0848	2.284E-3	3.0073	1406.5
2	4.8714	2.1811E-3	8.01	1416.7
3	4.4378	1.9932E-3	18.021	1432.7
4	4.2692	1.8854E-3	23.008	1442.1
5	4.9936	2.3249E-3	2.9999	1410.0
6	4.0955	1.7853E-3	28.097	1446.0
7	3.6486	1.644E-3	38.14	1463.2
8	3.384	1.4455E-3	48.031	1486.2
9	3.1876	1.3812E-3	53.297	1488.5
10	3.1247	1.2675E-3	58.074	1504.9

Table 3. Truncation errors for the expansion of the full Non-Linear AC model at order 1–4 (see Equations (17) and (18)), model evaluated at baseline potential −50 mV(Ag/AgCl)

NGM	T_2	T_3	T_4	T_5
1	0.0089242	0.0056758	3.0612E-8	2.9663E-10
2	0.0088153	0.0056712	3.3074E-8	3.3082E-10
3	0.0096438	0.0071791	3.2038E-8	3.1623E-10
4	0.0097004	0.00748	3.4635E-8	3.5257E-10
5	0.010127	0.0080942	3.1017E-8	3.0229E-10
6	0.010275	0.0083961	3.0832E-8	2.9986E-10
7	0.010568	0.0091685	3.2257E-8	3.1932E-10
8	0.010484	0.0092264	3.4933E-8	3.5667E-10
9	0.011488	0.011156	2.9182E-8	2.7836E-10
10	0.011541	0.011703	3.5206E-8	3.5986E-10

Table 4. Truncation errors for the expansion of the full Non-Linear AC model at order 1–4 (see Equations (17) and (18)), model evaluated at baseline potential −250 mV(Ag/AgCl)

NGM	T_2	T_3	T_4	T_5
1	0.072771	0.14288	3.6653E-8	3.6928E-10
2	0.076951	0.1491	3.5632E-8	3.5395E-10
3	0.08204	0.15599	3.5174E-8	3.4744E-10
4	0.08472	0.15973	3.497E-8	3.4423E-10
5	0.077642	0.15049	3.4417E-8	3.3689E-10
6	0.082729	0.15601	3.6891E-8	3.7239E-10
7	0.089964	0.16571	3.5453E-8	3.5254E-10
8	0.097475	0.17629	3.4438E-8	3.3725E-10
9	0.094902	0.17144	3.6531E-8	3.6846E-10
10	0.10092	0.18042	3.5362E-8	3.5E-10

results allow consideration of the TEI up to the third harmonic and then models with $m=3$ are employed.

We denote by $M_2(\omega,\mathrm{p})$ and $M_3(\omega,p)$ the magnitudes of the second and third harmonic terms Z_2 and Z_3 in Equation (15) and we evaluate the corresponding analytical models in all NGM sets in order to select the one yielding the lowest errors on the data of second and third harmonics, denoted H_2 and H_3, respectively (as represented in Figures 3 and 4). We considered higher harmonics normalized to their maxima because, owing to details of the electronic design of the modified FRA, it is not straightforward to define a common calibration factor for the absolute values of the impedance loci and of the higher harmonics, enabling us to use the absolute value of the latter quantities. Nevertheless an analytic model is of course available for the normalised higher harmonics. As a discrimination criterion for NGMs, we chose the estimate of the following relative errors in the 2-norm:

$$\mathrm{Err}_2=\frac{||H_2-M_2||_2^2}{||H_2||_2^2},\quad \mathrm{Err}_3=\frac{||H_3-M_3||_2^2}{||H_3||_2^2}. \qquad (19)$$

The functions $M_2(\omega;p)$ and $M_3(\omega;p)$ are plotted in Figures 3 and 4 as continuous lines; the curves corresponding to $\mathbf{p}_{NGM}$* are denoted by the symbol *. A reasonable agreement is found between the theoretical models M_2, M_3, evaluated at the 10 NGMs considered, and the experiment results H_2, H_3. It is worth stressing that the theoretical curves are not the result of a best fit procedure, but are deduced from the analytic expressions of the higher harmonics.

Table 5. Distances between experimental and theoretical values of the magnitudes of the 2nd and 3rd harmonics, evaluated at the 10 selected Numerical Global Minima (see Equation (19)); data corresponding to the experiments carried out with baseline potential of −50 mV(Ag/AgCl)

NGM	Err_2	Err_3
1	0.013994	0.040452
2	0.01291	0.037673
3	0.0089127	0.031378
4	0.0072994	0.027528
5	0.0068867	0.028029
6	0.0062114	0.026761
7	0.0042905	0.022093
8	0.003716	0.019781
9	0.0021766	0.016641
10	**0.0019738**	**0.011574**

The errors Err_2, Err_3 for each NGM of the two experiments are listed in Tables 5 and 6. The minimum errors for the experiments run at −50 and −250 mV vs Ag/AgCl are found to corresponds to the following two NGMs, respectively:

$\mathbf{p}^*_{\mathrm{NGM}}(-50\ \mathrm{mV})=[a_1, a_2, b_1, b_2]$
$=$ [1.2158 mA cm^{-2}, 1.2736×10^{-3} mA cm^{-2}, 113.54 mV dec^{-1}, 2188.6 mV dec^{-1}]
$\mathbf{p}^*_{\mathrm{NGM}}(-250\ \mathrm{mV})=[a_1, a_2, b_1, b_2]$
$=$[3.1247 mA cm^{-2}, 1.2675×10^{-3} mA cm^{-2}, 58.074 mV dec^{-1}, 1504.9 mV dec^{-1}]

Table 6. Distances between experimental and theoretical values of the magnitudes of the 2nd and 3rd harmonics, evaluated at the 10 selected Numerical Global Minima (see Equation (19)); data corresponding to the experiments carried out with baseline potential of −250 mV(Ag/AgCl)

NGM	Err_2	Err_3
1	0.38396	0.033484
2	0.35407	0.026219
3	0.31777	0.019462
4	0.30444	0.017402
5	0.33496	0.022163
6	0.32226	0.020675
7	0.26286	0.012874
8	0.23085	0.010909
9	0.23953	0.011448
10	**0.22179**	**0.010782**

Values of a_1 and b_1 are quite close to the values obtained by cyclic voltammetry in [1, 3]; the comments reported in this paper also apply for the corresponding reaction. The numerical values found for a_2 and b_2 are typical of a cathodically inhibited reaction, possibly implying a chemical rate determining step (e.g. [9]).

5. Conclusions

We report the first non-linear AC spectrometry experimental data applied to Cu electrodeposition from an acidic sulphate bath containing PEG. The impedance loci and the moduli of the second and third harmonic corresponding to two potentiostatic cathodic conditions were measured and analysed according to an earlier model [5]. The Numerical Global Minima [4] generated by Non-Linear Least-Squares fitting of the impedance locus were filtered with models for the second and third harmonic of the kinetic model. A single set of parameters satisfying the ensemble of non-linear models up to third order was extracted and can be regarded as a reliable approximation of the best fit of the kinetic model to the AC experiments.

References

1. B. Bozzini, C. Mele, L. D'Urzo, G. Giovannelli and S. Natali, *J. Appl. Electrochem.*, in press.
2. B. Bozzini, C. Mele and L. D'Urzo, *J. Appl. Electrochem.*, **36** (2006) 87.
3. E.E. Farndon, F.C. Walsh and S.A. Campbell, *J. Appl. Electrochem.* **25** (1995) 574.
4. I. Sgura and B. Bozzini, *Int. J. Non-Lin. Mech.* **40** (2005) 557.
5. B. Bozzini and I. Sgura, *Math. Prob. Eng.* in press.
6. D.D. Macdonald. *in* R. Varma and J.R. Selman (eds), Techniques for the Characterization of Electrodes and Electrochemical Processes, (John Wiley & Sons, NY, 1991), pp. 515.
7. A.R. Despić. *in* B.E. Conway, J.O'M. Bockris, E. Yeager, S.U.M. Khan and R.E. White (eds), Comprehension Treatise of Electrochemistry 7, (Plenum Press, NY, 1983), pp. 470.
8. MATLAB 6.5 Release 13- Optimisation Toolbox 2.2 – User's guide.
9. A.R. Despić and K. Popov. *in* R.E. White, B.E. Conway and J.O'M. Bockris (eds), Modern Aspects of Electrochemistry 7, (Plenum Press, NY, 1972), pp. 264.